PLASMA JET FOR FLOW CONTROL

N.V. Ardelyan, V.L. Bychkov*, D.V. Bychkov*, V.A. Chernikov,

K.V. Kosmachevskii and M.N. Sablin

Lomonosov Moscow State University, Moscow, Russia

**FSUE Moscow Radiotechnical Institute, Moscow, Russia, bychvl@orc.ru*

1. Introduction

The concept of plasma jets application for influence on a flow and gaseous fuels has been investigated in [1-2]. Calculations simulating gas discharge devices relate to composition of thermal plasmas in air, nitrogen and hydrogen as a function of gas temperature [3-4] show that for typical plasma jet temperatures in the range 3000-5000° K the conditions are already sufficient for influencing of plasma on a flow, and plasma dynamic processes becomes of interest from the point of view of applications for flow control. Especially they can be applicable for influence and creation of vortex structures and at impact of trailing wingtip vortex's parameters [5].

Solving this problem requires considering interaction of the plasma jet with a cross flow.

For this purpose we consider prospective to apply a magneto plasma compressor, which create a strong get with long penetration.

From a point of view of theoretical analysis we apply In a two-dimensional approach we model a row of plasma generators with the divergent nozzle interacting with the flow as we considered in [1-2].

2. Magneto-Plasma Compressor

Magneto plasma compressor, MPC, was specially designed to study interaction of supersonic airflow and plasma formations.

According to [6,7] data an initial velocity of plasma formation reaches 2 km/s and plasma parameters in a cumulating zone are the following: temperature is T= 18-20 $\times 10^3$ K and an electron concentration is n=5 $\times 10^{16}$ - 10^{17} cm^{-3}. Parameters of a power source were the next: charge capacity - 50 μF, voltage – 3 kV and it corresponds to 225 J of a stored energy. A duration of the first discharge current half- period was 20 μs (a duration of the first quasi period of a discharge current is approximately 50 μs). Photos of the discharges with and without airflow demonstrate the same pictures of airflow/plasma interaction and confirm that the penetration of the plasma does not depend on airflow velocity in these test conditions. The main near axis plasma part, its "core", keeps a propagation angle, both without a stream, and in it. The stream influence affects only a peripheral part of the stream which cross - section sizes considerably decrease as a result of the stream influence.

From the photos made at various pressure values in a receiver of the test gasdynamic channel stand, one can see, that the direction of the stream "core" propagation practically remains constants while the transversal sizes of peripheral area decrease, at that the more the greater is the pressure in the receiver. Besides, with pressure in the receiver increase the longitudinal sizes of the plasma stream decrease.

The undertaken experiments have shown that MPC discharge can be used for influence on a stream practically in all the volume of the supersonic air stream. It is necessary to notice, that duration of the MPC discharge is limited by a value size of an accumulation capacity and is of 50 - 150 μs.

Therefore the further experiments on research of MPC discharge applicability should include its studying in a pulse periodic mode and its increase in time of action.

3. Theoretical modeling

In a two-dimensional approach we model a row of plasma generators with the divergent nozzle interacting with the flow at some angle (0-180°) to the flow, see Fig.1.

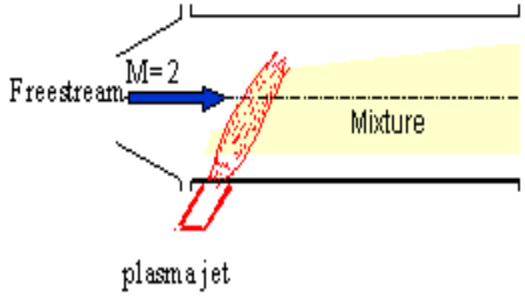

Fig.1. Plasma jet from a slot created by a row of plasma generators .

In this simulation as in [2,8], the gasdynamic equations are coupled with the 2-D Maxwell equations, and the plasma dynamics equations, accounting for ohmic heating and radiative plasma cooling. A Lagrange method based on a completely conservative implicit difference scheme with an adaptive triangular mesh [2,8] is applied. This was effective in modeling the coupling of the internal and external flows inside and outside the counterflow jet and its nozzle [2,8]. This approach is applied in this investigation of interaction of divergent plasma jets with cross flows.

Here we consider the construction of the plasma generator with the divergent inter electrode channel where the minimum nozzle diameter is 3 mm. The half angle is 6°. The nozzle length along the axis is 30 mm. The cathode diameter is 4.5 mm. The half angle of the conical cathode is 75°. The distance between the cathode to the nozzle is 1.7 mm. The transmitting area in channels is equal to the transmitting area in the nozzle critical cross section. In the initial part of the nozzle takes place the nitrogen inflow to the plasma generator. The range of the plasma generator power is 10-15 kW, the gas consumption range is 0.2 g/min-0.2 g/s. The energy input to the gas takes place mainly at a distance of 5 mm before the cathode.

The divergent plasma jet was chosen as reliable example of calculations compared with the data of experiments [9,10]

The model is based on the following system of radiating plasma electrodynamics equations verified in [1,2]

$$\partial\rho/\partial t + \mathrm{div}(\rho\mathbf{v}) = 0, \qquad (1)$$

$$\rho\, d\mathbf{v}/dt = -\,\mathbf{grad}\, p,$$

$$\rho\, d\varepsilon/dt = -\, p\, \mathrm{div}\, \mathbf{v} + j^2/\sigma - q,$$

$$\mathbf{rot}\, \mathbf{E} = -\,\partial\mathbf{B}/\partial t,$$

$$\mathbf{rot}\, \mathbf{B} = \mu_0\mathbf{j},$$

$$\mathrm{div}\, \mathbf{B} = 0,$$

$$\mathbf{j} = \sigma\, \mathbf{E},$$

where ρ, p, v, ε are the plasma (gas) density, pressure, velocity, and internal energy; σ is the electric conductance of the gas and plasma, q is the specific power of plasma thermal radiation, **E** is the electric field intensity, **B** is the magnetic field induction, **j** is the electric current density, and $\mu_0 = 4\pi\cdot 10^{-7}$ H/m. The unsteady cylindrically symmetrical approximation with respect to the gas and plasma rotation was applied: $\mathbf{v} = (v_r, v_\varphi, v_z)$, $\mathbf{B} = (0, B_\varphi, 0)$, $\mathbf{j} = (j_r, 0, j_z)$, $\mathbf{E} = (E_r, 0, E_z)$, $\partial/\partial\varphi = 0$; the subscripts r, φ, z correspond to the radial r, azimuth φ, and axial coordinate z. The plasma equation of state can be expressed as

$$p = \alpha\, \rho k_B T/m_{mol},\ \varepsilon = p/[\rho(\gamma - 1)], \qquad (2)$$

where γ is the adiabatic exponent, k_B is the Boltzmann constant, T is the plasma temperature, m_{mol} is the initial gas molecular mass, and factor α takes into account the free species number changes resulting from chemical reactions (primarily dissociation and ionization). Functions $\gamma = \gamma(p,T)$, $\alpha = \alpha(p,T)$, $\sigma = \sigma(p,T)$ and $q = q(p,T)$ for nitrogen plasmas were computed preliminarily and approximated on the basis of data in [3,4]. In calculations we firstly assumed $\alpha = 1.1$ and $\gamma = 1.4$, as in [1,2], but changed in subsequent in later parametric variations of the temperature T.

The computation region included both the regions inside the plasma generator and outside the model. No-slip boundary conditions on the walls were assumed for plasma and gas and $\partial/\partial r = 0$ was assumed on the axis of symmetry. The gas input azimuth and radial velocities $v_{\varphi 0}$, v_{r0} were determined via gas density ρ_0 from the given gas flow rate m' and areas of the inflow tangent orifices F_τ and of the circular input slot F_s: $v_{\varphi 0}$, $= m'/(\rho_0 F_\tau)$, $v_{r0} = m'/(\rho_0 F_s)$. The input gas temperature $T_0 = 300$ K. Conditions $p = p_f$, $v_z = -v_{zf}$, $T = T_f$ on the right-hand boundary defined the supersonic ambient flow. Conditions on the left-hand boundary and on the peripheral boundary provided a free exit of the fluid.

The entire left-hand wall inside the plasma generator had electric potential φ_1; in the slot where the gas is injected, the condition on the magnetic field defined via the total discharge current I was applied: $B_0 = \mu_0 I/(2\pi r_0)$, here r_0 is the corresponding radial coordinate. All the remaining walls had electric potential φ_2. Details of computations in case of internal problem are presented in[5]. To expedite the computations, a small background conductance $\sigma^* < 10^{-3}\,\sigma_{\max}$ was assumed to be in the cold gas; here $\sigma_{\max}$ is the highest value of plasma conductance in the electric current channel. The computed distribution of electric current in the rest of the channel proved to be practically independent of the fluctuations of the plasma conditions (see below). This is a result of the nitrogen weak plasma conductance dependence on plasma pressure and temperature in the parametric region of interest. This allowed us to "freeze" this distribution and to avoid its expensive recalculation during the computations. So we transformed the electrodynamic problem to the problem of the gas heating in the channel.

Special calculations were made on the divergent plasma generator injection to a gas at ($\theta = 180^0$). They are necessary to determine the distribution of parameters over the jet cross section at the outlet for the solution of the cross flow jet interaction at angles ($0 < \theta < 180^0$), conditions of [9-10]. In Fig 2-6 one can see the distribution of main parameters of the plasma entering the gas at ($\theta = 180^0$) the gas consumption 2 g/s. pressure of the oncoming flow P=0.2 atm. at the plasma generator power 15 kW, typical time in calculations 10^{-4} s. It is 2-D solution of the plasma-gas flow problem, including the internal and external problem as a whole. In this case we use the information on thermal conductivity and viscosity characteristics, since the temperatures in the plasma generator are high. As one can see the distribution of temperature, pressure and density is strongly non homogeneous over the nozzle's exit.

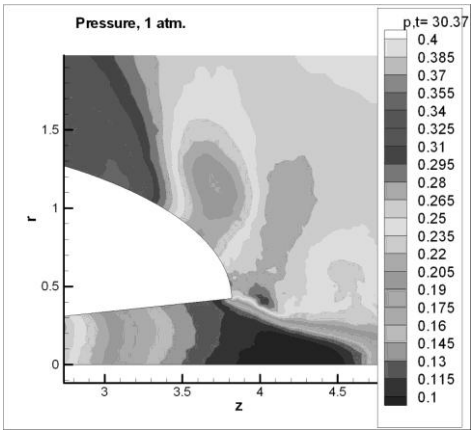

Fig.2. Pressure distribution at plasma jet entering the incident gas , consumption of a gas 0.2 g/s, inflowing gas pressure 0.2 atm, plasma generator power 15 kW, time $30 \cdot 10^{-4}$ s .

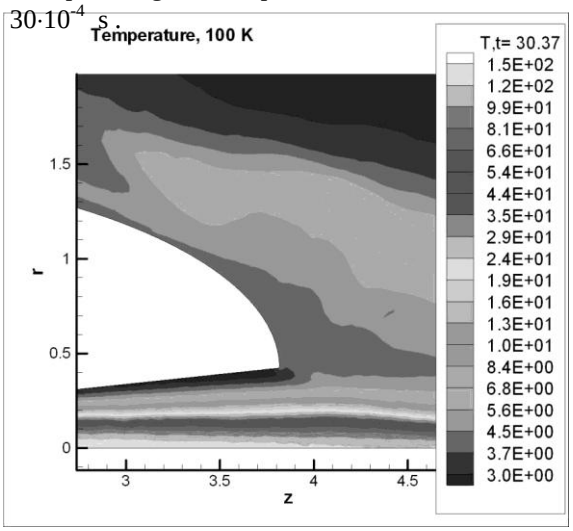

Fig.3. Temperature distribution at the plasma jet entering the incident gas, consumption of a gas 0.2 g/s, inflowing gas pressure 0.2 atm, plasma generator power 15 kW, time $30 \cdot 10^{-4}$ s .

Fig.4 Mach number distribution at the divergent plasma jet entering incident gas , consumption of a gas 0.2 g/s, inflowing gas pressure 0.2 atm, plasma generator power 15 kW, time $-30 \cdot 10^{-4}$ s .

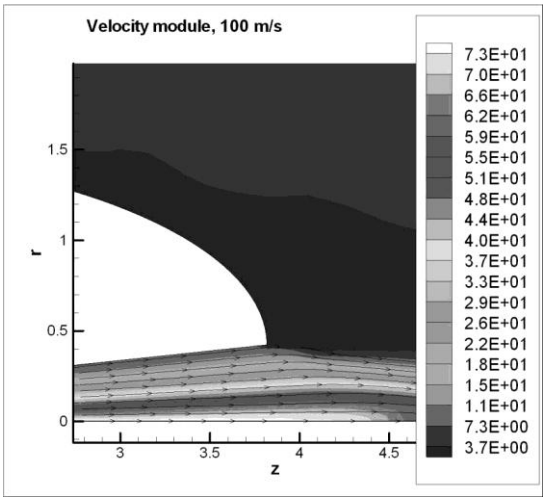

Fig.5. An absolute value of the velocity distribution at the plasma jet entering the incident gas, consumption of a gas 0.2 g/s, inflowing gas pressure 0.2 atm, plasma generator power 15 kW, time $30 \cdot 10^{-4}$ s .

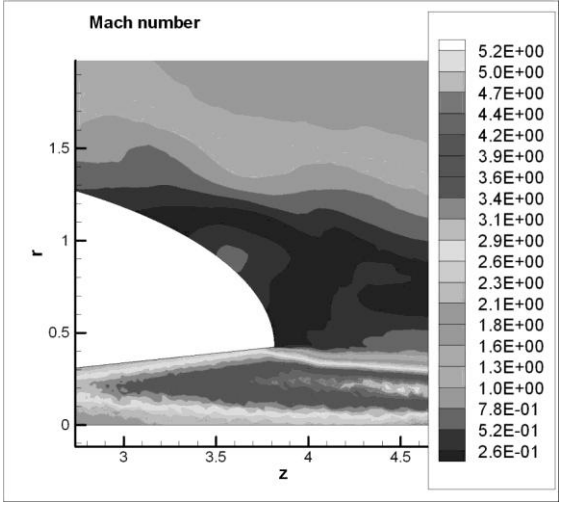

About 10 calculated points in the outlet channel cross section of the plasma generator were used for coupling plasma generator internal nozzle flow with the external flow as in our counterflow jet study [2].

In the solution of the jet-cross flow interaction at angles ($0<\theta<180^0$) the jet outside the plasma generator is considered to be flat, it models a row of nearby placed plasma generators. The parameters of the jet at the outlet to the cross flow are taken from the calculations for ($\theta=180^0$) [1]. Such a formulation allows to clarify characteristics of the jet interaction with the cross flow, spatial distribution of gas parameters distribution and peculiarities of the jet influence on oncoming flow (presence of shock waves, dependence on outflow angles).

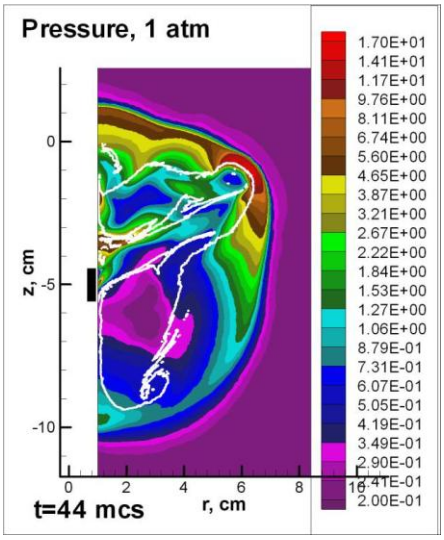

Fig.6. Plasma Jet interaction with the cross flow at ($\theta=135^0$). Pressure distribution at the plasma jet entering the incident gas, consumption of a gas 0.2 g/s, inflowing gas pressure 0.2 atm, plasma generator power 15 kW. White area is a boundary of the plasma region.

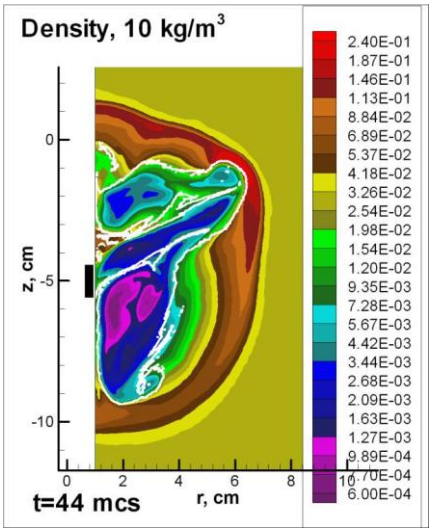

Fig.7. Plasma Jet interaction with the cross flow at ($\theta=135^0$). Density distribution at the plasma jet entering the incident gas, consumption of a gas 0.2 g/s, inflowing gas pressure 0.2 atm, plasma generator power 15 kW. White area is a boundary of the plasma region.

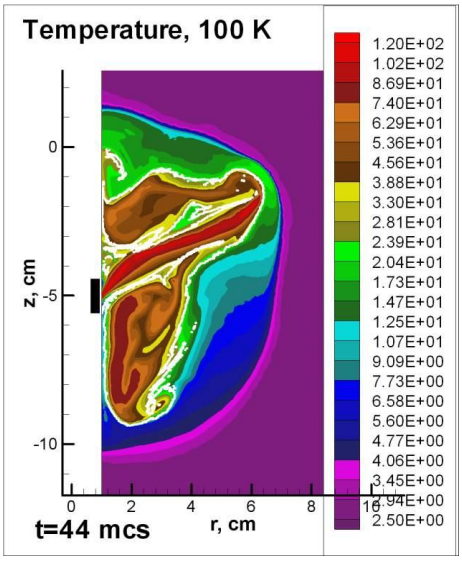

Fig.8. Plasma Jet interaction with the cross flow at ($\theta=135^0$). Temperature distribution at the plasma jet entering the incident gas, consumption of a gas 0.2 g/s, inflowing gas pressure 0.2 atm, plasma generator power 15 kW. White area is a boundary of the plasma region.

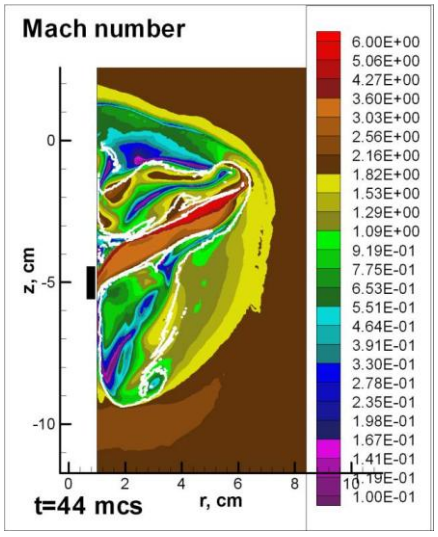

Fig.9. Plasma Jet interaction with the cross flow at ($\theta=135^0$). Mach number distribution at the plasma jet entering the incident gas, consumption of a gas 0.2 g/s, inflowing gas pressure 0.2 atm, plasma generator power 15 kW. White area is a boundary of the plasma region.

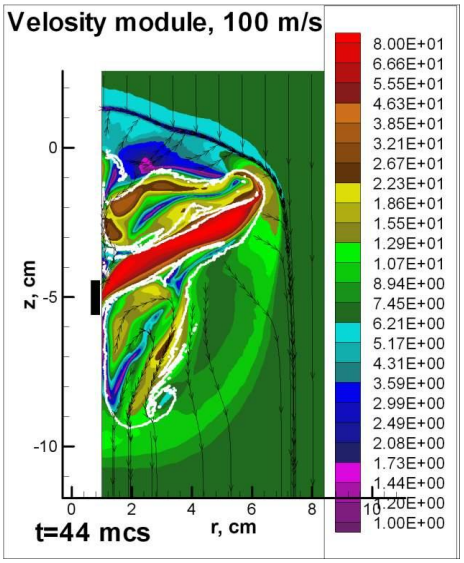

Fig.10. Plasma Jet interaction with the cross flow at ($\theta=135^0$). Absolute value of a velocity distribution at the plasma jet entering the incident gas, consumption of a gas 0.2 g/s, inflowing gas pressure 0.2 atm, plasma generator power 15 kW. White area is a boundary of the plasma region.

In this case we do not consider an influence of the viscosity and thermal conductivity outside the convergent nozzle in the cross flow since their influence at typical gasdynamic times and external temperatures is small.

Questions of turbulence are not considered on this study of investigations. In this studies we did not consider dissociated and charged plasma properties since this question has been analyzed in [2] it was shown there that nitrogen atom concentrations are of about 10^{18} cm^{-3}.

4. Discussion of obtained results

Results for three cases have been obtained.

Obtained results of the divergent plasma get parameters at injection to dead air qualitatively agree with the experimental data [9,10] in temperatures distribution (0.3 - ~45 kK) over the cross section at the same distance from the electrode and the same plasma generator power W~50 kW. Concentrations of electrons were comparable with those of [10].

In Fig.2-5 we present characteristics of the profiled plasma jet at the nozzle exit outflowing at 180° into nitrogen. Results of calculations show that at time moments $(4 - 10)\cdot 10^{-4}$ s quasi- stationary situation is realized.

In Fig. 6-10 we present results for a plasma jet coming out from the nozzle at ($\theta=135^0$). The jet screens a flow and a shock wave is formed in an oncoming flow. The oncoming flow turns at the shock and flows along the jet. A region screened by the jet is formed behind the jet. Temperature picture show appearance of a cluster of highly heated gas inside the plasma region.

Let us discuss possible force effects created by the plasma jets. N. Zhukovsky theorem determines a force influence of a potential flow on a flown around body of an arbitrary form. For example if a cylinder [11] is streamlined by an ideal incompressible liquid then it experiences a force action, normal to velocity in infinity V_∞ and equal to a product of this velocity a circulation $\Gamma = 2\cdot\oint \bar{V}\, d\bar{l}$ and a flow density ρ :

$$F = \rho\cdot\Gamma\cdot V_\infty\cdot l\,. \qquad (3)$$

Looking at the Fig.6-10, one can understand that jets greatly modify a flow around a surface creating additional lifting forces. They also create vortex structures which can modify trailing wingtip vortexes, and their influence will be greater than in case of dielectric barrier discharges, since the energy of jets is higher and their momentum is larger than those of DBD discharges [5]. The MPC plasma jets can be the best solution for creation of the plasma impact on the flow.

5. Summary and Conclusions

We have presented a preliminary experimental-theoretical analysis of a possible applicability of plasma jets to flow control problems. We have presented an effective type of plasma jets- magneto plasma compressor, experiments with which show its high penetration into a flow and the possibility of application in the flow control tasks.

We presented the external/internal theoretical-computation analysis of the plasma jet - crossflow interaction for conditions of already known and of planning experiments. Derived equations allowed application of the implicit free-Lagrange method to carry out computations. Our computations show the complex and non-homogeneous structure of the flow for the structure of a flow outside the plasma generator, which is different for different types of plasma generator geometries. Our results are in the qualitative agreement with results of known experiments for divergent plasma jets entering the dead gas. They facilitate interpretation of new experiments, particularly the relative roles of plasma and gasdynamic processes.

This preliminary analysis is necessary gasdynamic part of plasma- jet applicability for flow control investigation problems. Obtained results show that the plasma jet generators could be more prospectus for flow control of subsonic and supersonic streams than that considered in [5].

Acknowledgments

The authors wish to acknowledge EOARD program support under the Project # 2449 p.

References

1. Ardelyan N., Bychkov V., Chuvashev S., Kosmachevskii K. and Malmuth N. AIAA paper -2001-3101, *Proceedings 32nd AIAA Plasmadynamics and Lasers Conference and Fourth Weakly Ionized Gases Workshop*, 11-14 June 2001, Anaheim, CA.
2. Ardelyan N., Bychkov V., Kosmachevskii K. Solodovnikov N., Timofeev I., and Malmuth N. AIAA paper -2003-1191, 41 st AIAA Aerospace Aciences Meeting and Exhibit, 6-9 January 2003, Reno, Nevada.
3. Theory of thermal electric-arc plasmas. Ed. Prof. M.F. Zhukov, Prof. A.S. Koroteev. Novosibirsk. Nauka. 1987.
4. Zhukov M.F., Koroteev A.S., Uryukov B.A. Applied dynamics of thermal plasmas. Novosibirsk. Nauka. 1975.
5. Agibalova S.A., Golub V.V., Moralev I.A. Saveliev A.S.. The influence on trailing wingtip vortexes with a help of dielectric barrier discharge. Abstracts of the 11-th International Workshop on Magneto-plasma aerodynamics. Moscow April 10-12, 2012. P.11-12.
6. Chernikov A.V., Chernikov V.A., Chuvashev S.N., Ershov A.P., Shibkov V.M., TimofeevB.I, Timofeev I. B. "Crossed supersonic jets of a plasma and a dense gas". The 2nd Workshop on Magneto-plasma-aerodynamics in aerospace applications, 5-7 April 2000, Moscow, IHT of RAS, p.215-220.
7. Alexandrov A.F., Chernikov V.A., Chuvashev S.N., Ershov A.P., Shibkov V.M., Timofeev I.B. "Long-Lived Plasma Formations in Air". 9th International Space Planes and Hypersonic Systems and Technologies Conference, 1-4 November 1999, Norfolk, Virginia, USA, AIAA-99-4977.
8. Ardelyan N.V., Kosmachevskii K.V., Chuvashev S.N., Radiating Plasma Dynamics, Moscow, Energoatomizdat, 1991, P. 191-249.

9. Belevtsev A.A., Isakaev E.Kh., Markin A.V., and Chinnov V.F. Spectroscopic Analysis of Spatial Distribution of the Electron Temperature and Concentration in High-enthalpy flows of Argon and Nitrogen Plasma. High Temperature. 2002. V.40, No 1, P. 26-33.

10. Chinnov V.F. On a role of VUV radiation in near anode area of high current plasma generators with diverging anode channel. Teplofizika Vysokikh Temperatur. 2002. V.40, No 4, P. 533-543.

11. Kundu P.K., Cohen I.M., Dowling D.R. Fluid Mechanics. Academic Press. Elsevier. Amsterdam. Boston. 2012.